Zircon geochronology from the Kangaatsiaq–Qasigiannguit region, the northern part of the 1.9–1.8 Ga Nagssugtoqidian orogen, West Greenland

Kristine Thrane and James N. Connelly

The Kangaatsiaq–Qasigiannguit region in the northern part of the Palaeoproterozoic Nagssugtoqidian orogen of West Greenland consists of poly-deformed orthogneisses and minor occurrences of interleaved, discontinuous supracrustal belts. Laser ablation ICP-MS $^{207}Pb/^{206}Pb$ analyses of detrital zircons from four metasedimentary rocks (supplemented by ion probe analysis of one sample) and igneous zircons from six granitoid rocks cutting metasedimentary units indicate that the supracrustal rocks in the Kangaatsiaq–Qasigiannguit (Christianshåb) region are predominantly Archaean in age. Four occurrences of metasedimentary rocks are clearly Archaean, two have equivocal ages, and only one metasedimentary unit, from within the Naternaq (Lersletten) supracrustal belt, is demonstrably Palaeoproterozoic and readily defines a large fold complex of this age at Naternaq. The 2.9–2.8 Ga ages of detrital Archaean grains are compatible with derivation from the local basement orthogneisses within the Nagssugtoqidian orogen. The detrital age patterns are similar to those of metasediments within the central Nagssugtoqidian orogen but distinct from age patterns in metasediments of the Rinkian belt to the north, where there is an additional component of pre-2.9 Ga zircons. Synkinematic intrusive granitoid rocks constrain the ages of some Archaean deformation at 2748 ± 19 Ma and some Palaeoproterozoic deformation at 1837 ± 12 Ma.

Keywords: Nagssugtoqidian orogen, deformation, LA-ICP-MS, zircon, metasediment

K.T., *Geological Institute, University of Copenhagen, Øster Voldgade 10, DK-1350 Copenhagen K, Denmark.*
E-mail: *kthrane@geol.ku.dk*
J.N.C., *Department of Geological Science, University of Texas at Austin, Austin, TX 78712, USA.*

The Kangaatsiaq–Qasigiannguit area that is the focus of this paper (Fig. 1) forms a large part of the northern Nagssugtoqidian orogen, which is interpreted as the southern part of a major collisional orogenic system that crops out in central and northern West Greenland and adjacent parts of eastern Canada (Connelly *et al.* 2006). The northern Nagssugtoqidian orogen, which was re-investigated in 2001–2003 by the Geological Survey of Denmark and Greenland (GEUS) in co-operation with external partners, is underlain by poly-deformed, variably reworked grey Archaean orthogneiss interleaved with dismembered Archaean and Palaeoproterozoic supracrustal rocks of volcanic and sedimentary origin. Only few significant time marker horizons (such as distinct suites of mafic dykes or one or more groups of characteristic supracrustal rocks with known ages) are present. The primary objectives of this geochronological study were therefore to determine the extent of Palaeoproterozoic metasedimentary rocks and attempt to directly date different phases of deformation and metamorphism.

A number of lithological, structural and metamorphic features, especially in the Kangaatsiaq–Aasiaat area (Fig. 1),

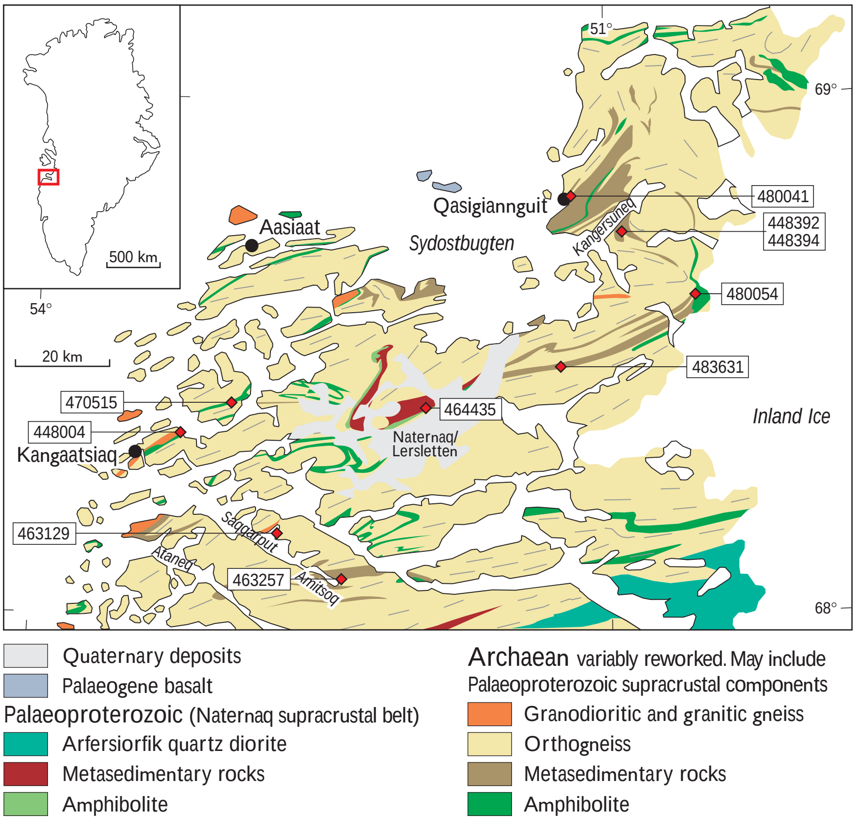

Fig. 1. Simplified geological map of the Kangaatsiaq–Qasigiannguit region, with sample locations.

provide some immediate constraints on the Archaean and Palaeoproterozoic geological evolution of the northern Nagssugtoqidian orogen, and are outlined here as an introduction to the geochronological study. The study area may be divided into two different tracts based on metamorphism and structural style (Piazolo *et al.* 2004; Mazur *et al.* 2006, this volume). The tract south-west and south-east of Kangaatsiaq is metamorphosed at granulite facies grade and is characterised by a general WSW–ENE-trending structural grain with large, moderately to steeply plunging fold structures and undeformed to weakly deformed, synkinematic granitic neosome (van Gool *et al.* 2002; Garde 2004). Several E–W-trending mafic dykes occur south of Kangaatsiaq around 68°N. They are undeformed and discordant to the main structures and lithological boundaries, but variably metamorphosed (Glassley & Sørensen 1980; Árting 2004). These dykes are presumed to be of Palaeoproterozoic age and perhaps related to pre-Nagssugtoqidian rifting (Árting 2004), and if so would constrain the deformation and granulite facies metamorphism south of Kangaatsiaq to be Archaean in age, whereas the thermal event recorded by the dykes themselves would be Palaeoproterozoic.

The remainder of the study area, to the north and east of Kangaatsiaq, is at amphibolite grade (e.g. Hollis *et al.* 2006, this volume), and does not display any signs of retrogression from granulite facies except within a *c.* 10 km thick transition zone adjacent to the granulite facies terrain. These northern and eastern areas generally possess a much more intense planar and linear tectonic fabric than in the south, commonly including a strong subhorizontal extension lineation that also penetrates the late granitic neosome. Furthermore, a structural discordance occurs in the Naternaq area (Fig. 1) between WNW–ESE-trending amphibolite to the west and the structurally overlying, NE–SW-trending Naternaq supracrustal belt in the east, suggesting that the respective structures of the two supracrustal units are unrelated to each other and of different age (Mazur *et al.* 2006, this volume). In addition, the northern and eastern areas also host occasional mafic dykes on islands north-east of Aasiaat and on the southern coast of Sydostbugten (Fig. 1). Although these dykes are still largely coherent and unmigmatised, they are intensely deformed, almost concordant with their host rocks, and tectonically thinned to about 1–2 m thick. Both the granitic neosome, the Naternaq supracrustal rocks, and the deformed dykes provide relative age constraints on the intense deformation in the northern and eastern parts of the study area. If it is again assumed that the deformed dykes in the north are Palaeoproterozoic, it would follow

Table 1. Zircon LA-ICP-MS ^{207}Pb-^{206}Pb data

448004 Metasediment NE of Kangaatsiaq

Spot	^{206}Pb (cps)	$^{207}Pb/^{206}Pb$	Age (Ma)	2σ %
1	22419	0.21046	2909	7.7
2	30428	0.20444	2862	4.9
3	27946	0.20011	2827	5.9
4	41739	0.20405	2859	4.8
5	66864	0.20548	2870	5.8
6	52963	0.20846	2894	4.2
7	70422	0.18216	2673	3.9
8	46147	0.20058	2831	5.2
9	73807	0.20449	2862	3.7
10	41046	0.20919	2899	5.9
11	75396	0.20183	2841	6.5
12	84403	0.20242	2846	4.2
13	27932	0.20390	2858	7.5
14	102678	0.20107	2835	6.0
15	129026	0.18972	2740	6.9
16	46526	0.20716	2883	5.5
17	71802	0.20579	2873	6.3
18	659551	0.20033	2829	4.9
19	165828	0.19242	2763	6.1
20	73874	0.19895	2818	5.4
21	20371	0.18508	2699	5.5
22	21982	0.17386	2595	5.3
23	33164	0.21021	2907	6.4
24	86486	0.18406	2690	5.1
25	99148	0.20434	2861	4.4
26	54554	0.20049	2830	5.6
27	52435	0.17947	2648	3.8
28	45325	0.20018	2828	4.3
29	75391	0.18983	2741	3.0
30	77047	0.20775	2888	4.7
31	32181	0.19856	2814	3.1
32	50218	0.19811	2811	3.3
33	28491	0.20148	2838	4.3
34	21801	0.19768	2807	4.6
35	22466	0.20144	2838	5.9
36	48990	0.20013	2827	3.3
37	26535	0.20445	2862	5.8
38	114112	0.18364	2686	2.1
39	41973	0.20083	2833	3.4
40	57549	0.20210	2843	2.6
41	26869	0.25312	3204	2.7
42	49986	0.19811	2811	3.0
43	20567	0.19924	2820	4.6
44	5467	0.19417	2778	9.2
45	29042	0.20106	2835	4.2
46	9255	0.18565	2704	6.7
47	18597	0.20277	2849	4.3
48	112700	0.17900	2644	2.3
49	84858	0.19285	2767	2.8
50	14867	0.17617	2617	8.2
51	24908	0.19765	2807	3.7
52	11178	0.19419	2778	5.5
53	91255	0.17807	2635	4.3
54	28338	0.20395	2858	4.7
55	24855	0.18937	2737	4.8
56	7761	0.18757	2721	9.0
57	12436	0.19563	2790	6.5
58	12571	0.19849	2814	5.4

448392 Granite, Kangersuneq

Spot	^{206}Pb (cps)	$^{207}Pb/^{206}Pb$	Age (Ma)	2σ %
1	318831	0.19069	2748	3.5
2	361175	0.18986	2741	2.7
3	406129	0.19945	2822	3.3
4	163666	0.18800	2725	3.6
5	205935	0.19380	2775	3.1
6	227282	0.19148	2755	3.0
7	123658	0.18830	2727	3.1
8	294942	0.18738	2719	5.1
9	407109	0.19415	2778	5.0
10	481882	0.19342	2771	5.1
11	212302	0.18706	2716	4.7
12	407464	0.19766	2807	3.0
13	491512	0.19950	2822	4.2
14	94032	0.18905	2734	3.0
15	173984	0.18392	2689	4.9
16	109933	0.18320	2682	5.7
17	50994	0.19030	2745	4.6
18	13465	0.18864	2730	6.2
19	21101	0.17697	2625	6.4
20	99478	0.18431	2692	5.8
21	108982	0.18687	2715	3.9
22	33255	0.18969	2739	5.7
23	192965	0.18985	2741	6.8
24	280376	0.18859	2730	6.1
25	287725	0.18761	2721	5.1
26	101087	0.18975	2740	4.7
27	85412	0.18695	2716	4.3
28	125421	0.18639	2711	6.2
29	45496	0.18854	2730	5.7
30	75470	0.18108	2663	4.9
31	40021	0.18483	2697	4.9
32	48564	0.19087	2750	5.6
33	101631	0.18754	2721	3.2
34	117730	0.18292	2679	2.5
35	49211	0.18807	2725	3.8
36	112930	0.18847	2729	2.9
37	202637	0.18826	2727	2.2
38	102831	0.18893	2733	2.2
39	55266	0.19174	2757	2.8
40	45349	0.18639	2711	4.5
41	104416	0.18742	2720	3.3
42	188642	0.18481	2696	2.2
43	97849	0.18797	2724	2.6
44	145946	0.17859	2640	4.0

448394 Metasediment, Kangersuneq

Spot	^{206}Pb (cps)	$^{207}Pb/^{206}Pb$	Age (Ma)	2σ %
1	695411	0.16006	2456	3.6
2	52863	0.20417	2860	5.3
3	443404	0.11180	1829	3.8
4	1104248	0.11717	1913	4.4
5	579803	0.11532	1885	4.7
6	231966	0.12351	2008	4.9
7	362937	0.10979	1796	3.1
8	303451	0.11334	1854	3.9
9	277637	0.11090	1814	3.1
10	380962	0.12251	1993	3.9
11	115636	0.16115	2468	6.0
12	461330	0.11598	1895	3.5
13	493717	0.19532	2787	3.7
14	207687	0.17408	2597	5.3
15	393460	0.11112	1818	2.7
16	242631	0.10929	1788	4.9
17	132013	0.19838	2813	4.9
18	178574	0.10859	1776	6.1
19	303683	0.10774	1762	4.1
20	241139	0.15569	2409	7.4
21	51484	0.12627	2047	5.5
22	53211	0.12080	1968	7.7
23	53531	0.11660	1905	6.9
24	23896	0.19593	2793	6.2
25	79706	0.11458	1873	6.4
26	89308	0.11277	1845	6.3
27	63147	0.11176	1828	8.6
28	12586	0.19431	2779	6.5
29	100961	0.13800	2202	7.0
30	12592	0.16853	2543	9.7
31	57066	0.11124	1820	8.5
32	51764	0.11438	1870	10.1
33	218430	0.11295	1847	7.4
34	78169	0.10868	1777	9.7
35	96773	0.11345	1855	8.4
36	143102	0.11037	1806	6.7
37	33237	0.13986	2225	6.4
38	92186	0.10819	1769	9.7
39	80332	0.12802	2071	8.3
40	35510	0.19386	2775	8.0
41	11684	0.18283	2679	7.4
42	21389	0.19620	2795	8.2
43	14702	0.19528	2787	9.7
44	19762	0.19659	2798	6.5
45	36375	0.11197	1832	9.0
46	17548	0.18024	2655	11.7
47	9064	0.19962	2823	10.9
48	11530	0.19199	2759	7.8
49	64234	0.11111	1818	10.3
50	7566	0.16671	2525	11.0
51	38371	0.10619	1735	9.1
52	15464	0.18496	2698	9.1
53	15534	0.14855	2329	9.3
54	27618	0.11461	1874	8.4
55	15853	0.19890	2817	9.4
56	10902	0.18316	2682	11.0
57	8905	0.20952	2902	9.4
58	6493	0.18680	2714	10.5
59	16248	0.19267	2765	8.7
60	43736	0.14480	2285	6.4
61	48133	0.11266	1843	12.3
62	52656	0.12037	1962	10.7
63	88558	0.11566	1890	7.2
64	65717	0.10988	1797	8.8
65	14964	0.15276	2377	8.5
66	59777	0.11635	1901	7.3
67	23849	0.16781	2536	8.6
68	16825	0.19548	2789	12.3
69	17260	0.14321	2266	8.8
70	28538	0.19178	2757	10.3
71	65355	0.11192	1831	8.4
72	58939	0.12654	2050	9.6
73	69509	0.11151	1824	6.8
74	49893	0.13319	2140	8.6
75	76541	0.11448	1872	8.1
76	67611	0.11351	1856	8.0
77	58817	0.10691	1747	8.9
78	69641	0.11468	1875	11.3
79	57943	0.11116	1818	4.7

463129 Synkinematic granite, Saqqarput

Spot	^{206}Pb (cps)	$^{207}Pb/^{206}Pb$	Age (Ma)	2σ %
1	2283739	0.18759	2721	3.0
2	1266859	0.19890	2817	3.6
3	344375	0.18904	2734	4.1
4	531257	0.18883	2732	5.5
5	565174	0.19441	2780	4.6
6	247679	0.18844	2729	4.9
7	460352	0.20656	2879	3.8
8	1058356	0.19510	2786	3.2
9	405853	0.18296	2680	6.8
10	554081	0.17660	2621	3.0
11	1363965	0.20876	2896	4.0
12	935603	0.19609	2794	2.7
13	605520	0.18625	2709	2.6
14	516471	0.17880	2642	5.1
15	822166	0.18954	2738	5.5
16	655511	0.20436	2861	4.0
17	755390	0.19587	2792	5.0
18	127005	0.18594	2707	5.9
19	422927	0.19261	2765	4.8
20	653950	0.19183	2758	4.0
21	1135912	0.19679	2800	2.9
22	1096015	0.19497	2785	2.4
23	653314	0.19170	2757	2.6
24	228993	0.20892	2897	7.4
25	221510	0.21878	2972	9.2
26	346159	0.20045	2830	6.6
27	37048	0.16944	2552	11.9
28	97269	0.17974	2650	10.8
29	85210	0.18521	2700	8.7
30	172975	0.18213	2672	8.2
31	171017	0.17446	2601	9.0
32	165639	0.18002	2653	5.5
33	133709	0.18851	2729	7.8
34	182742	0.18315	2682	5.2
35	125199	0.18194	2671	7.0
36	169034	0.19244	2763	7.5
37	85182	0.16778	2536	9.4

Table 1 *(continued)*

Spot	^{206}Pb (cps)	^{207}Pb/^{206}Pb	Age (Ma)	2σ %
38	101924	0.18113	2663	7.6
39	178145	0.20233	2845	8.9
40	35771	0.18557	2703	8.3
41	23866	0.19033	2745	10.0
42	78620	0.22740	3034	11.3
43	88660	0.20740	2885	7.8
44	264622	0.18784	2723	6.5
45	219347	0.19029	2745	5.2
46	215885	0.18648	2711	9.4
47	117234	0.17897	2643	9.0
48	29425	0.18849	2729	8.9
49	59458	0.18317	2682	10.0
50	44706	0.19343	2772	11.5
51	47511	0.20920	2899	14.7
52	52220	0.18199	2671	10.6
53	58597	0.17855	2639	12.7
54	47047	0.18403	2690	6.8
55	85100	0.19408	2777	8.0
56	150838	0.18512	2699	9.1
57	42220	0.18152	2667	8.4
58	182300	0.17444	2601	6.3
59	181857	0.19158	2756	5.8
60	656182	0.18446	2693	3.8
61	1625878	0.19433	2779	4.0
62	1033362	0.19004	2742	7.1

463257 Metasediment, Amitsoq

Spot	^{206}Pb (cps)	^{207}Pb/^{206}Pb	Age (Ma)	2σ %
1	94060	0.20316	2852	4
2	126332	0.19611	2795	4
3	245874	0.21538	2946	4
4	154787	0.20172	2840	4
5	68216	0.19982	2825	4
6	428099	0.18536	2701	4
7	100464	0.18737	2719	4
8	106081	0.19619	2794	4
9	178863	0.20711	2883	4
10	72018	0.19715	2808	4
11	102336	0.18203	2671	4
12	218440	0.21010	2907	4
13	144435	0.20135	2837	4
14	73200	0.20617	2875	4
15	103837	0.17190	2575	4
16	100257	0.15132	2361	4
17	120574	0.20468	2864	4
18	88636	0.20786	2889	4
19	129707	0.20434	2861	4
20	133092	0.21288	2928	4
21	176443	0.20885	2897	4
22	48385	0.19377	2774	5.2
23	61486	0.19210	2760	8.2
24	60275	0.22028	2983	3.6
25	44550	0.20247	2846	6.8
26	30952	0.20191	2842	5.9
27	7392	0.18113	2663	8.0
28	20571	0.19351	2772	8.6
29	15357	0.19909	2819	6.7
30	31747	0.20691	2881	7.0
31	22596	0.20038	2829	8.1
32	35613	0.20326	2853	7.7
33	15204	0.20568	2872	10.5
34	24804	0.19424	2778	8.2
35	17027	0.19728	2804	5.8
36	21866	0.19494	2784	8.4
37	13148	0.20815	2891	9.3
38	27502	0.20821	2892	6.1
39	26648	0.20452	2863	8.3
40	27263	0.18701	2716	10.7
41	46499	0.14869	2331	6.7
42	36471	0.20245	2846	6.7
43	64587	0.20102	2834	8.7
44	31986	0.20332	2853	8.9
45	46174	0.21292	2928	8.9
46	61284	0.20775	2888	6.6
47	41436	0.20439	2862	6.8
48	72510	0.20430	2861	5.1
49	67124	0.20347	2854	7.9
50	37221	0.19866	2815	7.0

464435 Metasediment, Naternaq

Spot	^{206}Pb (cps)	^{207}Pb/^{206}Pb	Age (Ma)	2σ %
1	620630	0.12031	1961	4
2	184109	0.14293	2261	4
3	177844	0.12013	1959	4
4	508546	0.12356	2019	4
5	521502	0.11208	1833	4
6	560514	0.11545	1887	4
7	455565	0.10976	1795	4
8	294092	0.11916	1944	4
9	407244	0.12342	2006	4
10	217026	0.11556	1889	4
11	240050	0.11948	1948	4
12	285058	0.12258	1995	4
13	651523	0.11831	1938	4
14	367681	0.12552	2036	4
15	337595	0.12582	2041	4
16	465635	0.11732	1917	4
17	321964	0.12267	1995	4
18	1150971	0.11774	1922	4
19	266990	0.12383	2013	4
20	374761	0.12502	2030	4
21	297903	0.12321	2002	4
22	87395	0.11806	1927	4.3
23	88706	0.12335	2005	6.5
24	53359	0.13734	2194	6.5
25	72472	0.11727	1915	5.8
26	16174	0.13058	2106	4.4
27	125924	0.11860	1935	4.6
28	81398	0.11940	1947	6.3
29	93208	0.11402	1864	6.3
30	131504	0.12001	1956	4.2
31	107212	0.12410	2016	6.6
32	66177	0.12687	2055	7.7
33	72338	0.11608	1897	4.1
34	163168	0.11450	1872	4.4
35	92298	0.12172	1982	5.5
36	220614	0.12305	2001	4.3
37	112247	0.12249	1993	5.7
38	76097	0.11662	1905	4.7
39	76847	0.11907	1942	4.1
40	39338	0.11918	1944	6.8
41	51130	0.11856	1935	6.6
42	86970	0.12690	2055	5.0
43	128237	0.11865	1936	5.3
44	47126	0.12236	1991	5.5
45	84328	0.11894	1940	5.6
46	307611	0.12127	1975	5.0
47	115975	0.11797	1926	6.9
48	149629	0.12005	1957	7.5
49	385671	0.11759	1920	7.7
50	454534	0.12076	1967	6.8
51	245715	0.11875	1937	7.4
52	320479	0.12160	1980	6.4
53	1098422	0.10860	1776	7.8
54	578352	0.12047	1963	4.1
55	186864	0.11804	1927	7.0
56	79299	0.11614	1898	5.5
57	255968	0.10900	1783	3.3
58	707747	0.11876	1938	7.4
59	97872	0.12173	1982	6.5
60	109798	0.11649	1903	5.4
61	489175	0.12003	1957	4.0

470515 Pegmatite NE of Kangaatsiaq

Spot	^{206}Pb (cps)	^{207}Pb/^{206}Pb	Age (Ma)	2σ %
1	149998	0.11231	1837	3.3
2	114249	0.11111	1818	2.3
3	128681	0.11066	1810	2.5
4	249115	0.11405	1865	2.5
5	174468	0.11307	1849	2.2
6	188664	0.11253	1841	2.7
7	118304	0.11223	1836	3.0
8	69708	0.11414	1866	4.3
9	107108	0.11379	1861	3.5
10	57749	0.11019	1803	5.2
11	255076	0.11091	1814	2.7
12	112190	0.11350	1856	4.7
13	145495	0.11459	1873	3.2
14	162431	0.11214	1834	4.2
15	42424	0.11157	1825	5.5
16	109374	0.11367	1859	4.3
17	52552	0.11218	1835	6.4
18	67018	0.11372	1860	5.2
19	38574	0.11173	1828	5.3
20	184531	0.11162	1826	2.5
21	420598	0.11279	1845	2.5
22	675700	0.11206	1833	1.7

480041 Quartz diorite, Qasigiannguit

Spot	^{206}Pb (cps)	^{207}Pb/^{206}Pb	Age (Ma)	2σ %
1	130744	0.19864	2815	5.2
2	127784	0.19639	2796	4.7
3	30286	0.19684	2800	4.6
4	28769	0.20120	2836	4.7
5	41484	0.19738	2805	4.7
6	19837	0.20222	2844	7.0
7	35270	0.19516	2786	5.5
8	48190	0.20117	2836	5.6
9	35231	0.19155	2756	5.0
10	93023	0.19849	2814	4.8
11	36116	0.19465	2782	4.8
12	82370	0.19490	2784	10.4
13	58322	0.19959	2823	7.2
14	61328	0.19932	2821	6.7
15	58943	0.19951	2822	11.6
16	25024	0.19642	2797	3.7
17	61436	0.19260	2765	5.7
18	56976	0.19778	2808	7.2
19	43379	0.19673	2799	5.3
20	68466	0.19216	2761	7.7

480054 Tonalite intruding mafic complex

Spot	^{206}Pb (cps)	^{207}Pb/^{206}Pb	Age (Ma)	2σ %
1	8174	0.20380	2857	10.3
2	10419	0.19353	2772	7.4
3	18592	0.20474	2864	5.5
4	213185	0.15919	2447	5.9
5	17238	0.19681	2800	5.3
6	11204	0.20444	2862	6.4
7	17603	0.20266	2848	7.2
8	36568	0.20791	2889	9.5
9	42107	0.20580	2873	6.5
10	30492	0.19888	2817	7.1
11	25591	0.20251	2847	7.2
12	14106	0.20374	2856	6.4
13	18218	0.20025	2828	4.4
14	20117	0.19869	2816	5.8
15	42704	0.20836	2893	6.8
16	29583	0.20336	2853	7.6
17	23900	0.19738	2805	9.0

483631 Granite intruding metasediment

Spot	^{206}Pb (cps)	^{207}Pb/^{206}Pb	Age (Ma)	2σ %
1	259347	0.19195	2759	3.1
2	155094	0.19256	2764	2.4
3	94380	0.19393	2776	3.3
4	33706	0.18539	2702	3.7
5	57040	0.18930	2736	3.2
6	42007	0.19204	2760	3.5
7	71104	0.19592	2793	3.8
8	33803	0.19616	2794	4.1
9	79316	0.19110	2752	3.9
10	13550	0.18486	2697	7.3
11	57313	0.19407	2777	4.3
12	56128	0.19155	2756	3.1
13	56620	0.19591	2792	3.4
14	101430	0.19250	2764	3.6
15	41779	0.19211	2760	3.4
16	367814	0.19593	2793	2.0
17	118779	0.18771	2722	2.7
18	26473	0.16345	2492	13.9
19	45218	0.19626	2795	3.6
20	76399	0.19586	2792	3.6
21	24409	0.18865	2730	4.7

Table 2. Zircon ion probe U-Th-Pb data from sample 464435, Naternaq

Spot #	U ppm	Th ppm	Pb ppm	Th/U measured	f^{206} %	$^{207}Pb/^{206}Pb$	σ %	$^{207}Pb/^{235}U$	σ %	$^{206}Pb/^{238}U$	σ %	Disc. % (conv.)	Ages (Ma) $^{207}Pb/^{206}Pb$	σ	$^{207}Pb/^{235}U$	σ	$^{206}Pb/^{238}U$	σ
1	404	161	167	0.40	0.37	0.1160	0.36	5.390	1.81	0.3370	1.77	–1.4	1898	6	1935	16	1970	30
2	384	170	170	0.44	0.02	0.1162	0.33	5.727	1.80	0.3575	1.77	4.4	1894	13	1875	17	1858	29
3	235	121	101	0.51	1.34	0.1159	0.75	5.338	1.93	0.3341	1.78	–2.2	1911	6	1898	16	1886	29
4	411	178	173	0.43	0.24	0.1170	0.33	5.483	1.81	0.3398	1.77	–1.5	1892	6	1906	16	1918	29
5	489	195	208	0.40	0.24	0.1158	0.32	5.534	1.80	0.3466	1.77	1.6	1916	6	1902	16	1890	29
6	360	123	149	0.34	0.02	0.1174	0.33	5.511	1.80	0.3406	1.77	–1.6	1895	6	1906	16	1917	29
7	416	163	176	0.39	0.04	0.1160	0.31	5.537	1.80	0.3463	1.77	1.3	1909	6	1921	16	1932	30
8	413	178	178	0.43	0.03	0.1169	0.31	5.629	1.80	0.3494	1.77	1.4	1860	7	1775	15	1704	27
9	653	281	239	0.43	0.70	0.1137	0.40	4.743	1.82	0.3025	1.77	–9.5	1901	7	1901	16	1900	29
10	237	88	99	0.37	0.04	0.1163	0.39	5.500	1.81	0.3429	1.77	0.0	1896	7	1883	16	1872	29
11	239	108	101	0.45	0.05	0.1174	0.39	5.521	1.81	0.3410	1.77	–1.6	1918	7	1904	16	1891	29
12	448	224	194	0.50	0.03	0.1170	0.39	5.539	1.81	0.3434	1.77	–0.5	1911	7	1907	16	1903	29
13	2192	1713	975	0.78	0.15	0.1165	0.17	5.337	1.78	0.3323	1.77	–3.3	1903	3	1875	15	1849	2

Errors on ratios and ages are quoted at 1σ level.
f^{206} %: The fraction of common ^{206}Pb, estimated from the measured ^{204}Pb.
Disc. % (conv.): Degree of discordance of the zircon analysis (at the centre of the error ellipse).

that the northern and eastern parts of the study area are strongly reworked by Nagssugtoqidian deformation and amphibolite facies metamorphism.

Geochronological targets and methods

Both Archaean and Palaeoproterozoic supracrustal sequences are known to exist within the Nagssugtoqidian orogen (Marker *et al.* 1999; Nutman *et al.* 1999). Depositional ages of such supracrustal belts may be constrained by the ages of detrital zircons in their sedimentary components, since the youngest grains define their maximum age of deposition; conversely, the age of a magmatic rock that has intruded the supracrustal sequence may serve to define a lower depositional age limit. Ideally, both metasediment and cross-cutting magmatic rocks from the same outcrop should be analysed to best constrain the timing of deposition. However, cross-cutting intrusive rocks of appropriate age (i.e. other than late Palaeoproterozoic pegmatites) were not generally present. The direct dating of Archaean or Palaeoproterozoic deformation by dating e.g. synkinematic granitoids requires the rather scarce occurrence of an intrusive rock that unequivocally both cuts and is affected by a single fabric.

Ten samples from the Kangaatsiaq–Qasigiannguit area, mainly provided by members of the GEUS mapping groups in 2001–2002, have been analysed by quadrupole laser ablation inductively coupled mass spectrometry (LA-ICP-MS) at the University of Texas at Austin (zircon Pb-Pb data, Table 1); additional ion probe U-Pb zircon data from one metasedimentary rock were obtained at the NORDSIM laboratory, Naturhistoriska Riksmuseet, Stockholm (Table 2). Analytical details are given in the appendix. The samples were collected from seven different, dismembered metasedimentary sequences (four samples of metasediment and four samples of cross-cutting granitoid rocks), and from intrusive granite and orthogneiss that constrain the timing of deformation (two samples). All ages of rocks presented in this manuscript have been calculated using Isoplot/Ex (Ludwig 1999) and are reported with 2-sigma uncertainties.

The main advantage of using the LA-ICP-MS technique for zircon geochronology is that each analysis only lasts about two minutes, whereas the analytical time on an ion microprobe is typically around 15–20 minutes. This becomes an important factor when analysing detrital rocks, where analysis of a large number of detrital grains is essential to achieve good statistics. The major limitation of the LA-ICP-MS technique employed is that U-Pb ratios could not be measured, and only $^{207}Pb/^{206}Pb$ ages are obtained. A direct indication of concordance therefore is not available, and all the ages obtained should be interpreted conservatively to represent minimum ages of crystallisation or metamorphism. Furthermore, common Pb corrections cannot be carried out due to interference in the plasma of ^{204}Hg from the carrier gases. A test of the LA-ICP-MS instrument used in this study was carried out by Connelly *et al.* (2006), who analysed zircons from the Itilli diorite, Disko Bugt, West Greenland using both LA-ICP-MS and ID-TIMS methods and found that the $^{207}Pb/^{206}Pb$ age of 3019 ± 23 Ma obtained with the laser instrument compared well with its ID-TIMS age of 3030 +8/–5 Ma.

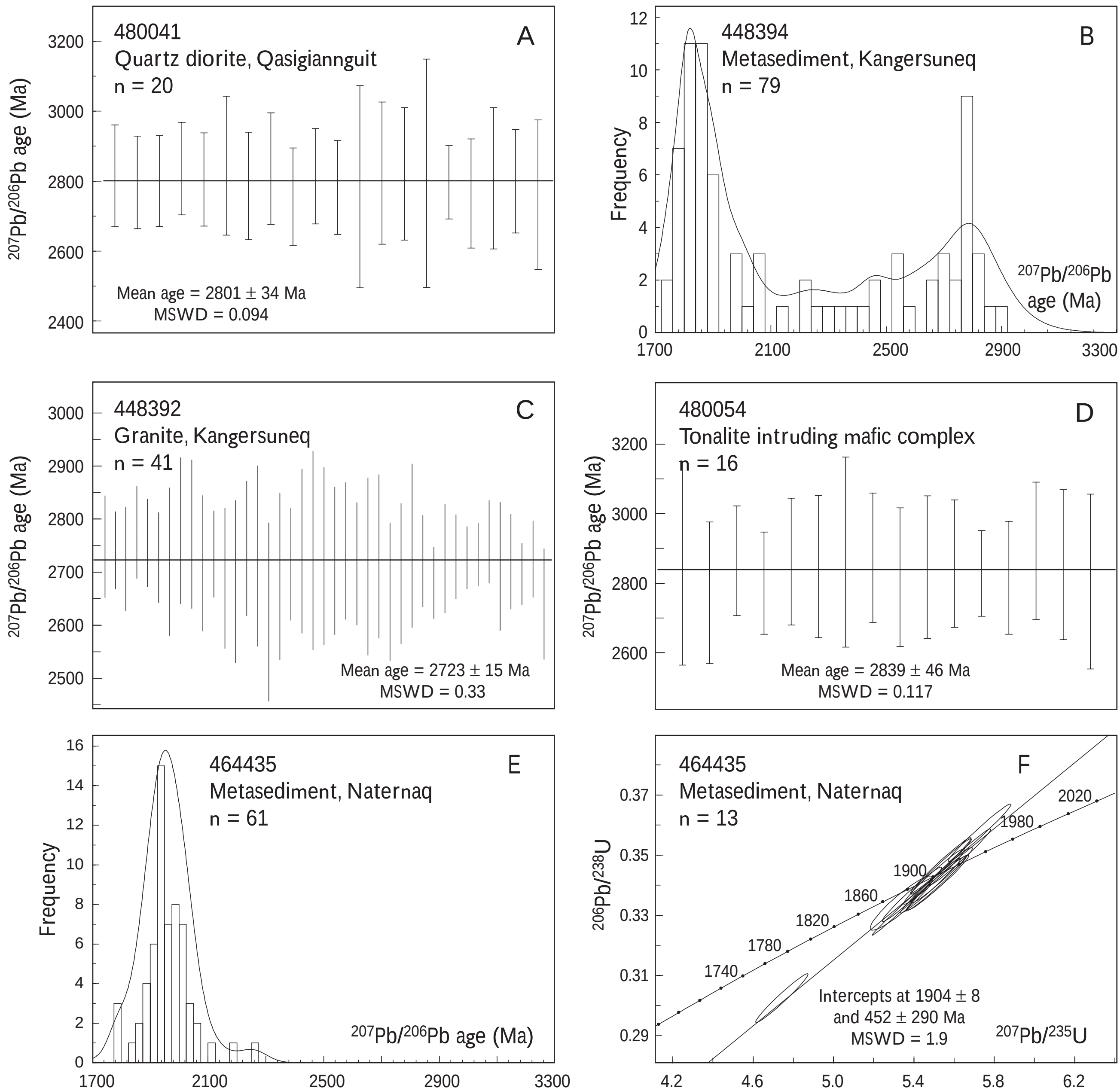

Fig. 2. Zircon age data from the Kangaatsiaq–Qasigiannguit region. A, C, D, G, J, K: Weighted average plots of LA-ICP-MS $^{207}Pb/^{206}Pb$ age data of igneous rocks. B, E, H, I: Probability density plots of LA-ICP-MS $^{207}Pb/^{206}Pb$ age data of metasediments. F: Ion probe U-Pb age data (concordia plot), sample 464435.

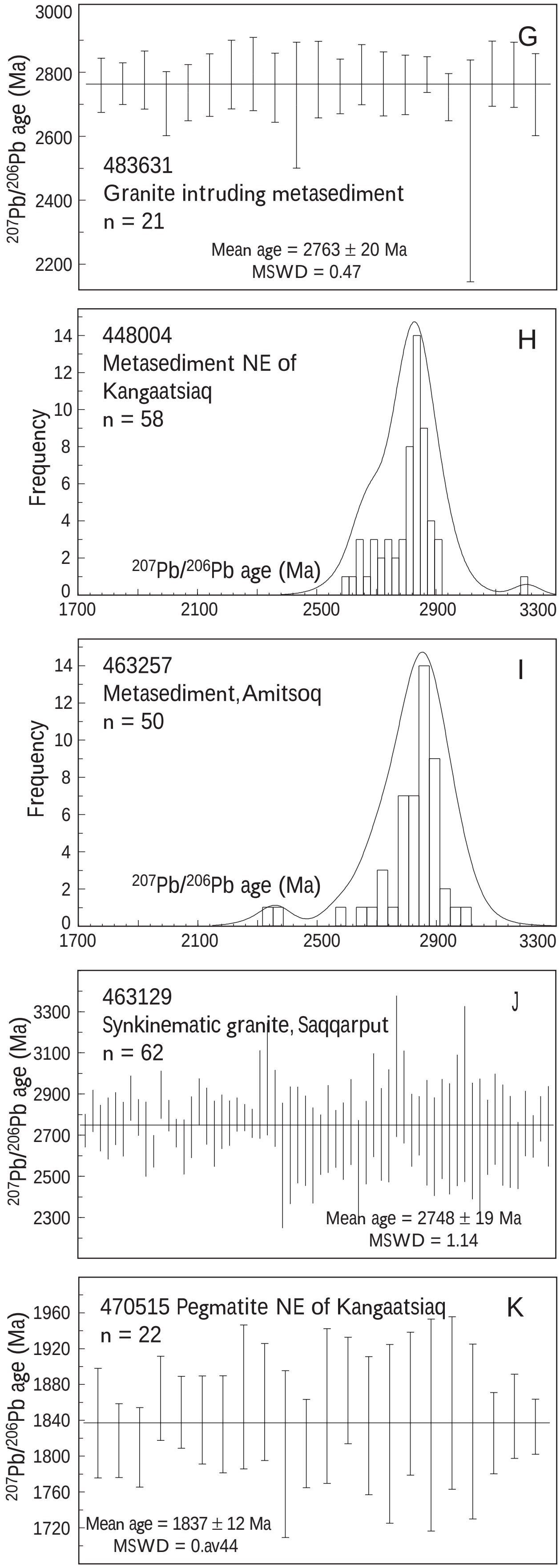

Geochronological age constraints of metasedimentary belts

The study area contains numerous, dismembered, discontinuous belts of metasedimentary rocks that may be either Archaean or Palaeoproterozoic in age. While the main focus of this work was to constrain their timing of deposition, provenance information gained through the detrital zircons permits regional correlation of these metasedimentary belts. The analysed samples are presented in Tables 1–2 and Fig. 2 and discussed below from north to south.

Sample 480041, quartz diorite intruding metasedimentary and metavolcanic rocks at Qasigiannguit

Sample 480041 of a homogeneous, grey, medium-grained quartz diorite was collected 3 km east of Qasigiannguit at 68°48.83′N, 51°08.05′W (Fig. 1). The rock consists of plagioclase, quartz, hornblende and biotite and has a strong linear fabric. The quartz diorite forms a 3–4 km long elongate body exposed on the top of the ridge facing Qasigiannguit. Its contact relationships are generally equivocal due to deformation, but at the south-western margin the contact appears to be intrusive into a metasedimentary-metavolcanic sequence.

The zircons from this sample are clear and stubby. Twenty grains were analysed, which yield consistent $^{207}Pb/^{206}Pb$ ratios corresponding to a weighted mean age of 2801 ± 34 Ma (MSWD = 0.094, Fig. 2A). The age is interpreted as the crystallisation age of the quartz diorite, implying that the supracrustal sequence it cuts must also be Archaean.

Samples 448394, metasediment and 448392, intruding granite on the south coast of Kangersuneq

Sample 448394 (68°46.24′N, 50°52.16′W) from a pelitic metasedimentary rock and sample 448392 (68°46.20′N, 50°51.55′W) of a granite that cuts the metasedimentary belt, were collected *c.* 200 m apart on the south coast of Kangersuneq (Fig. 1). After the analytical results were obtained, the locality was revisited in 2003 and the previously reported field relations confirmed (Jeroen van Gool, personal communication 2003).

The zircons from the metasediment are brownish, elongate, 100–200 µm long, and in many cases cracked and showing clear signs of dissolution. The least altered and, presumably, least disturbed zircons were chosen for analyses. In several cases it was possible to distinguish broad rims containing more U than the cores, and in such cases both core and rim were analysed. Seventy-nine spots were analysed and yield an age spectrum with a large peak at 1850 Ma and a smaller one at 2800 Ma (Fig. 2B). A range of intermediate ages (2500–2100 Ma) between the two peaks are also present (see below). The Archaean peak comprises only analyses from cores, whereas the 1850 Ma peak consists of analyses from both cores and rims.

The zircons from the granite are typically brown, and larger than those in the metasediment. In size they range from 100–350 µm and occur both as slender and somewhat stubby crystals. Core–rim zonation is observed in the majority of the zircons. Of 44 grains analysed from the granite, 41 yielded a consistent pattern of $^{207}Pb/^{206}Pb$ ratios corresponding to an average age of 2723 ± 15 Ma (MSWD = 0.33) (Fig. 2C); both cores and rims were analysed in several grains without observing any age variations. The remaining three grains yield ages from 2822 to 2807 Ma and are most likely inherited. Due to the homogeneity of the zircon population it is highly unlikely that the zircons are detrital grains inherited from the metasediment. They are also unlikely to have been inherited from the orthogneisses adjacent to the metasediment, as these do not generally contain such young zircons. Therefore, the age of 2723 ± 15 Ma is interpreted as the emplacement age of the granite, and the metasediment must also be of Archaean age. The 1850 Ma peak for the zircons in the metasediment is therefore interpreted to date Nagssugtoqidian metamorphism, and the 2500–2100 Ma ages most likely represent Archaean zircons that have suffered Pb-loss; alternatively the latter analyses might represent accidental mixtures of cores and rims.

Sample 480054, tonalite intruding mafic complex *c.* 25 km south-east of Kangersuneq

Sample 480054, a biotite-hornblende tonalite, was collected from a relatively undeformed tonalitic body *c.* 2 km^2 in size at 68°35.53′N, 50°30.28′W within a large mafic supracrustal complex near the Inland Ice about 25 km south-east of Kangersuneq (Fig. 1). The tonalite is light grey in colour, medium- to coarse-grained, homogeneous, and has a weak linear fabric. It is feldspar-phyric with phenocrysts up to 2 cm in diameter. Near the contacts with the surrounding mafic rocks the tonalite contains xenoliths of the mafic supracrustal rocks, and its intrusive nature is unequivocal. Dykes of tonalite, 50 cm to 2 m wide, extend from the main tonalite body into rocks of the surrounding large mafic complex.

The tonalite sample yielded a population of large, euhedral, mostly prismatic, clear to yellow zircons. Seventeen spots on zircon grains were analysed, and sixteen of them generated a consistent spectrum of $^{207}Pb/^{206}Pb$ ratios corresponding to an average age of 2839 ± 46 Ma (MSWD = 0.117) (Fig. 2D). The consistent $^{207}Pb/^{206}Pb$ ratios indicate that little or no Pb-loss has occurred. The age result is therefore interpreted to closely reflect the crystallisation age of the tonalite, and the mafic complex intruded by the tonalite must consequently also be Archaean.

Sample 464435, metasedimentary rock from the Naternaq supracrustal belt

Naternaq (Lersletten) is an extensive Quaternary outwash plain with scattered outcrops of Precambrian basement gneisses and supracrustal rocks (Østergaard *et al.* 2002). A sample of very fine-grained mica schist was collected from the extensive Naternaq supracrustal belt at 68°24.10′N, 51°56.70′W (Fig. 1). The zircons are elongate, 50–150 µm long, and vary in colour from clear to slightly brown. All 61 analyses carried out yield Palaeoproterozoic $^{207}Pb/^{206}Pb$ ages ranging from 2261 to 1776 Ma, with the main peak of $^{207}Pb/^{206}Pb$ ages around 1950 Ma (Fig. 2E). While it is possible that some of the younger grains may be metamorphic, we interpret the majority of the grains to be detrital because of the igneous appearance of the zircons and because they are older than any metamorphic event so far described in the Nagssugtoqidian orogen (e.g. Connelly *et al.* 2000, earliest metamorphism at *c.* 1870 Ma). Furthermore, it seems unlikely that a zircon population from a metasedimentary rock would only comprise metamorphic grains and not contain a single detrital grain. Consequently this requires a Palaeoproterozoic deposition age for the metasedimentary unit at Naternaq.

In order to confirm the obtained $^{207}Pb/^{206}Pb$ LA-ICP-MS ages, zircons from this sample were also analysed on the CAMECA IMS 1270 ion microprobe at the NORDSIM Laboratory, Swedish Museum of Natural History, Stockholm. The thirteen ion probe analyses yield a cluster of ages on the concordia diagram of Fig. 2F (Table 2), with an upper intercept isochron age of 1904 ± 8 Ma (MSWD = 1.9). The ion probe age is thus slightly younger than the *c.* 1950 Ma peak obtained by LA-ICP-MS, but the two data sets overlap within the large analytical error of the latter method, and the apparent older LA-ICP-MS age could be due to common Pb for which we were unable to correct. In conclusion, the ion probe data clearly demonstrate that the zircons are older than any metamorphic ages hitherto obtained from the Nagssugtoqidian orogen. The most likely interpretation is that the sediment at Naternaq was derived from the magmatic arc that formed in the central part of the orogen between 1920 and 1870 Ma (Kalsbeek *et al.* 1987; Kalsbeek & Nutman 1996; Whitehouse *et al.* 1998; Connelly *et al.* 2000). The new age data from the Naternaq supracrustal belt have important consequences for the structural interpretation of the Naternaq area, documenting the existence of large Palaeoproterozoic folds.

Sample 483631, granite vein intruding metasediment on strike with the Naternaq supracrustal sequence

A sample (483631) of an 8 cm wide vein of muscovite-biotite granite vein was collected east of Naternaq at 68°31.04′N, 51°17.87′W (Fig. 1). The granite vein is deformed but clearly intrudes mica schist on strike with the eastern part of the Naternaq supracrustal belt.

Most of the zircons in sample 483631 are long, prismatic grains with a distinct core-rim zonation and range from clear to brownish in colour. Twenty-two analyses were carried out, mostly on cores, but also on a few rims. All except one analysis yielded consistent $^{207}Pb/^{206}Pb$ ratios corresponding to an average age of 2763 ± 20 Ma (MSWD = 0.47, Fig. 2G). One core analysis yielded a $^{207}Pb/^{206}Pb$ age of 2467 ± 158 Ma, which may be due to Pb-loss. The analyses demonstrate that the granite is Archaean. The regional basement does not generally contain orthogneisses with such young ages and, therefore, limits the possibility that the zircons in the granite were inherited. It follows that the supracrustal rocks east of Naternaq on strike with the Naternaq supracrustal belt must also be of Archaean age.

Sample 448004, metasedimentary belt near Kangaatsiaq

Sample 448004 of a quartz-rich metasedimentary rock was collected north-east of Kangaatsiaq at 68°21.15′N, 53°13.18′W (Fig. 1). The zircons vary from elongate to stubby but all have been rounded during transport. They are clear and between 50 to 200 µm in length. A weak igneous zonation is present in the majority of the grains. Fifty-eight spots were analysed, and both core and rim were analysed in several grains. The age population ranges from 2909 to 2595 Ma, with a single grain yielding an age of 3200 Ma (Fig. 2H). A peak is present around 2850 Ma, which is a common age for polyphase orthogneisses within the Nagssugtoqidian orogen (Kalsbeek *et al.* 1987; Kalsbeek & Nutman 1996; Whitehouse *et al.* 1998; Connelly & Mengel 2000; Hollis *et al.* 2006, this volume). The scatter of younger ages from 2800 to 2595 Ma most likely results from variable degrees of Pb loss. We cannot with certainty assign an age of deposition to this sediment, as the data are compatible with both Archaean and Palaeoproterozoic sedimentation.

Sample 463257, quartz-rich metasedimentary sequence at Amitsoq

Sample 463257 of a medium- to fine-grained, quartz-rich metasedimentary rock with abundant small garnets was collected at the head of the fjord Amitsoq at 68°05.78′N, 52°30.99′W (Fig. 1). It is part of an extensive metasedimentary sequence, which is significantly more quartz-rich than all other metasedimentary rocks reported from the Kangaatsiaq map area, although similar rocks have been observed in the central Nagssugtoqidian orogen (Jeroen van Gool, personal communication 2003).

The zircons are clear, 50–250 µm in length and vary from elongate to stubby, and have been rounded during transport. Most zircons show clear igneous zonation, and some contain a high-U metamorphic rim. This rim was unfortunately too thin to analyse with the LA-ICP-MS. All except two of the 50 analysed grains yield Archaean ages, with two exceptions interpreted to have suffered Pb-loss. The zircons show very little age variation, with a major peak of $^{207}Pb/^{206}Pb$ ages at around 2850 Ma (Fig. 2I). This age is comparable to that of the surrounding regional orthogneisses, and indicates that the detritus may be locally derived. However, it is only possible to conclude that the sediment was deposited after 2850 Ma.

Dating of deformation using synkinematic granitic rocks

Sample 463129, synkinematic granite vein at Saqqarput

A sample of synkinematic granite (463129) was collected at Saqqarput at 68°09.22′N, 52°42.65′W (Fig. 1). The granite occurs as fine- to medium-grained, subconcordant veins in the orthogneiss. Sixty-two analyses yielded $^{207}Pb/^{206}Pb$ ratios corresponding to an average $^{207}Pb/^{206}Pb$ age of 2748 ± 19 Ma (MSWD = 1.14; Fig. 2J). This is interpreted to be the crystallisation age of the granite since, as in sample 483631 described above, it is unlikely that zircons of this age are inherited. Some of the observed deformation in the host basement orthogneisses must, therefore, also be Archaean in age.

Sample 470515, pegmatite north-east of Kangaatsiaq

A sample of pegmatite (470515) was collected north-east of Kangaatsiaq at 68°20.23′N, 59°00.17′W (Fig. 1). The pegmatite forms a 020° trending vertical sheet cutting orthogneiss. The pegmatite is a member of a conjugate set of pegmatites within the Kangaatsiaq map area that indicate late, regional N–S orientated compression (Ian Alsop, personal communication 2002), and itself contains evidence of ductile sinistral shear along its margins; the regional foliation is deflected into sinistral shear fabrics, indicating that the pegmatite emplacement took place later than the foliation formation in the gneisses, but while the host rock was still hot enough to behave in a ductile manner.

The sample contains large, brownish, prismatic zircons that vary from slender to short and stubby in shape. Twenty-two spots were analysed on thirteen grains. Both rims and cores were analysed on several grains, but no age variation was documented between the two. All analyses yield the same result within uncertainties; the average $^{207}Pb/^{206}Pb$ ratio corresponds to an age of 1837 ± 12 Ma (MSWD = 0.44) (Fig. 2K). This is interpreted to be the emplacement age of the pegmatite, and is considered to date the late Nagssugtoqidian N–S compression.

Discussion and conclusions

The zircon ages obtained from this study show that metasedimentary rocks in the Kangaatsiaq–Qasigiannguit region are predominately Archaean in age. The best age constraints come from the four Archaean granitoid rocks that cut four different supracrustal belts. Only one metasediment was analysed from these belts and yields an Archaean detrital peak of *c.* 2800 Ma and a Palaeoproterozoic peak of *c.* 1850 Ma. The Palaeoproterozoic peak is attributed to the growth of metamorphic zircon during Nagssugtoqidian metamorphism. Similarly, the occurrences of ages between 2800–1850 Ma are attributed to Pb-loss from detrital grains and/or mixed analysis of detrital and metamorphic zircon. Two of the three remaining metasedimentary rocks yield only Archaean detrital ages with peaks between 2800 and 2900 Ma, which are similar to the ages of the basement orthogneisses in the Nagssugtoqidian orogen (Kalsbeek *et al.* 1987; Kalsbeek & Nutman 1996; Whitehouse *et al.* 1998; Connelly & Mengel 2000) and may indicate that the sedimentary sequences were derived from local sources. While it is tempting to conclude that these metasediments might also themselves be of Archaean age, the lack of cross-cutting granites from these locations only permits the conclusion that they must be younger than 2850 Ma. Thus, the sediments could have been deposited either in the Archaean at around 2850–2750 Ma (i.e., before the regional 2.75 Ga metamorphism documented within the Nagssugtoqidian orogen), or during the Palaeoproterozoic (most likely before the formation of the Arfersiorfik–Sisimiut arc; Kalsbeek *et al.* 1987; Kalsbeek & Nutman 1996; Whitehouse *et al.* 1998; Connelly *et al.* 2000).

The remaining sample of metasediment (464435), collected from the Naternaq supracrustal belt, is the only metasediment in this study which is interpreted to be of Palaeoproterozoic age. Similar rocks which crop out south of Sydostbugten to the north-east have previously been interpreted as along-strike equivalents of the Naternaq supracrustal belt, although the intervening area is partly concealed by Quaternary deposits (Fig. 1). However, the discordant Archaean granitic vein (483631) that cuts the metasedimentary rocks south of Sydostbugten requires that the two belts contain rocks of different age.

It is interesting to note that all the Archaean detrital ages obtained match the ages between 2850 and 2800 Ma of the Archaean basement gneisses in the central Nagssugtoqidian orogen. This distinguishes the metasedimentary rocks of the study area from metasedimentary rocks in the Rinkian belt to the north, which include detrital zircons that are as old as 3600 Ma (Thrane *et al.* 2003).

The predominance of Archaean metasedimentary rocks unfortunately precludes them from being useful marker horizons to partition Archaean and Palaeoproterozoic deformation. Nevertheless, the 2748 ± 19 Ma synkinematic granite (463129) from Saqqarput south-east of Kangaatsiaq dates large fold structures in the northern Nagssugtoqidian basement at around this age, which overlaps with the previously defined age of Archaean deformation and metamorphism in the central part of the orogen (e.g. Connelly & Mengel 2000).

The new age data place several constraints on the timing and style of Palaeoproterozoic metamorphism and deformation in the region. The Palaeoproterozoic sediment at Naternaq (sample 464435) was probably metamorphosed and deformed shortly after its deposition, in line with the significant *c.* 1850 Ma metamorphic peak in the Archaean sediment from Kangersuneq (sample 448394). The metamorphic zircon age from this sample is not very precise, and TIMS analyses would be necessary to obtain an exact age of the metamorphism. However, it correlates with previous estimates for the timing of deformation and metamorphism both north and south of the study area (Kalsbeek *et al.* 1987; Kalsbeek & Nutman 1996; Whitehouse *et al.* 1998; Connelly *et al.* 2000; Thrane *et al.* 2003; Connelly *et al.* 2006). Furthermore, a late phase of N–S-directed shortening is dated at 1837 ± 12 Ma by a synkinematic pegmatite (470515). The age of this pegmatite may correlate with the 1821 Ma D2 deformation event defined in the central Nagssugtoqidian orogen by Connelly *et al.* (2000), and with 1821–1823 Ma deformation east of Ilulissat in the north (Connelly *et al.* 2006).

Acknowledgements

Funding by the Carlsberg Foundation (Thrane) and the National Science Foundation (grant EAR-0337594 to Connelly) is gratefully acknowledged. We thank Ian Alsop (University of St. Andrews), Adam A. Garde and Jeroen van Gool (GEUS) for providing samples. We also thank John Lansdown (The University of Texas at Austin) for assisting in collecting the LA-ICP-MS data, and Julie A. Hollis and Adam A. Garde (GEUS) for re-analysing sample 464435 zircons on the ion microprobe. Allen P. Nutman and Åke Johansson are thanked for their constructive comments, and Adam A. Garde and A.K. Higgins are thanked for help with the geological introduction.

References

Árting, U.E. 2004: A petrological study of basic dykes and sills of assumed Palaeoproterozoic age in central western Greenland, 122 pp., two appendices. Unpublished M.Sc. thesis, University of Copenhagen, Denmark.

Connelly, J.N. & Mengel, F.C. 2000: Evolution of Archean components in the Nagssugtoqidian orogen, West Greenland. Geological Society of America Bulletin 112, 747–763.

Connelly, J.N., van Gool, J.A.M. & Mengel, F.C. 2000: Temporal evolution of a deeply eroded orogen: the Nagssugtoqidian orogen, West Greenland. Canadian Journal of Earth Sciences 37, 1121–1142.

Connelly, J.N., Thrane, K., Krawiec, A.W. & Garde, A.A. 2006: Linking the Palaeoproterozoic Nagssugtoqidian and Rinkian orogens through the Disko Bugt region of West Greenland. Journal of the Geological Society (London) 163, 319–335.

Garde, A.A. 2004: Geological map of Greenland, 1:100 000, Kangaatsiaq 68 V.1 Syd. Copenhagen: Geological Survey of Denmark and Greenland.

Glassley, W.E. & Sørensen, K. 1980: Constant *Ps*-*T* amphibolite to granulite facies transition in Agto (West Greenland) metadolerites: implications and applications. Journal of Petrology 21, 69–105.

Hollis, J.A., Keiding, M., Stensgaard, B.M., van Gool, J.A.M. & Garde, A.A. 2006: Evolution of Neoarchaean supracrustal belts at the northern margin of the North Atlantic Craton, West Greenland. In: Garde, A.A. & Kalsbeek, F. (eds): Precambrian crustal evolution and Cretaceous–Palaeogene faulting in West Greenland. Geological Survey of Denmark and Greenland Bulletin 11, 9–31 (this volume).

Kalsbeek, F. & Nutman, A.P. 1996: Anatomy of the Early Proterozoic Nagssugtoqidian orogen, West Greenland, explored by reconnaissance SHRIMP U-Pb dating. Geology 24, 515–518.

Kalsbeek, F., Pidgeon, R.T. & Taylor, P.N. 1987: Nagssugtoqidian mobile belt of West Greenland: a cryptic 1850 Ma suture between two Archaean continents – chemical and isotopic evidence. Earth and Planetary Science Letters 85, 365–385.

Ludwig, K.R. 1999: Isoplot/Ex version 2.00 – A geochronological toolkit for Microsoft Excel. Berkeley Geochronology Center, Special Publication 2.

Marker, M., Whitehouse, M., Scott, D., Stecher, O., Bridgwater, D. & van Gool, J.A.M. 1999: Deposition, provenance and tectonic setting for metasediments in the Palaeoproterozoic Nagssugtoqidian orogen, West Greenland: a key for understanding crustal collision. Abstracts EUG 10, Strasbourg, France.

Mazur, S., Piazolo, S. & Alsop, G.I. 2006: Structural analysis of the northern Nagssugtoqidian orogen, West Greenland: an example of complex tectonic patterns in reworked high-grade metamorphic terrains. In: Garde, A.A. & Kalsbeek, F. (eds): Precambrian crustal evolution and Cretaceous–Palaeogene faulting in West Greenland. Geological Survey of Denmark and Greenland Bulletin 11, 163–178 (this volume).

Nutman, A.P., Kalsbeek, F., Marker, M., van Gool, J.A.M. & Bridgwater, D. 1999: U-Pb zircon ages of Kangâmiut dykes and detrital zircons in metasediments in the Palaeoproterozoic Nagssugtoqidian orogen (West Greenland): clues to the pre-collisional history of the orogen. Precambrian Research 93, 87–104.

Østergaard, C., Garde, A.A., Nygaard, J., Blomsterberg, J., Nielsen, B.M., Stendal, H. & Thomas, C.W. 2002: The Precambrian supracrustal rocks in the Naternaq (Lersletten) and Ikamiut areas, central West Greenland. Geology of Greenland Survey Bulletin 191, 24–32.

Piazolo, S., Alsop, G.I., van Gool, J. & Nielsen, B.M. 2004: Using GIS to unravel high strain patterns in high grade terranes: a case study of indentor tectonics from West Greenland. In: Alsop, G.I. *et al.* (eds): Flow processes in faults and shear zones. Geological Society Special Publication (London) 224, 63–78.

Schuhmacher, M., de Chambost, E., McKeegan, K.D., Harrison, T.M. & Migeon, H. 1994: In situ dating of zircon with the CAMECA ims 1270. In: Benninghoven, A. (ed.): Secondary Ion Mass Spectrometry SIMS IX, 919–922. Chichester: Wiley.

Thrane, K., Connelly, J.N., Garde, A.A., Grocott, J. & Krawiec, A. 2003: Linking the Palaeoproterozoic Rinkian and Nagssugtoqidian belts of central W. Greenland: implications of new U-Pb and Pb-Pb ages. European Union of Geosciences Meeting, Geophysical Research Abstracts, CD 5, Abstract # 09275.

van Gool, J.A.M. *et al.* 2002: Precambrian geology of the northern Nagssugtoqidian orogen: mapping in the Kangaatsiaq area. Geology of Greenland Survey Bulletin 191, 13–23.

Whitehouse, M.J., Claesson, S., Sunde, T. & Vestin, J. 1997: Ion microprobe U-Pb zircon geochronology and correlation of Archaean gneisses from the Lewisian Complex of Gruinard, north-western Scotland. Geochimica et Cosmochimica Acta 61, 4429–4438.

Whitehouse, M.J., Kalsbeek, F. & Nutman, A.P. 1998: Crustal growth and crustal recycling in the Nagssugtoqidian orogen of West Greenland: constraints from radiogenic isotope systematics and U-Pb zircon geochronology. Precambrian Research 91, 365–381.

Wiedenbeck, M., Allé, P., Corfu, F., Griffin, W.L., Meier, M., Oberli, F., von Quardt, A., Roddick, J.C. & Spiegel, W. 1995: Three natural zircon standards for U-Th-Pb, Lu-Hf, trace element and REE analyses. Geostandards Newsletter 19, 1–23.

Williams, I.S. 1998: U-Th-Pb geochronology by Ion Microprobe. In: McKibben, M.A., Shanks III, W.C. & Ridley, W.I. (eds): Applications of microanalytical techniques to understanding mineralising processes. Reviews in Economic Geology 7, 1–35.

Manuscript received 15 October 2004; revision accepted 9 September 2005

Appendix

Analytical methods

Rock samples were crushed to mineral size under clean conditions using a jaw crusher and a disc pulveriser, and initial mineral separation was made using a Wilfley table at the University of Copenhagen or the University of Texas at Austin. All subsequent procedures, including sieving, heavy liquids and magnetic separation, were conducted at the University of Texas at Austin. Mineral fractions were characterised using a binocular reflected light microscope, a transmitted light petrographic microscope (with condenser lens inserted to minimise edge refraction), and a scanning cathodoluminescence (CL) imaging system on a JEOL 730 scanning electron microscope. Selected zircons of comparable size were hand picked and placed on two-sided tape, collared, and covered with epoxy. The zircons in the resulting mount were ground to approximately two thirds of their original thickness and polished. CL imaging was used to characterise the zircons before analysis.

Laser ablation analysis utilised a Merchantek 213nm YAG-laser connected to a Micromass quadrupole mass spectrometer (Platform). Fractionation and inherent detector non-linearity were accounted for by analysing zircons already well characterised by TIMS. Corrections necessary to obtain the correct $^{207}Pb/^{206}Pb$ ratios for these internal laboratory standards, covering a range of intensities and isotopic ratios, were applied to unknowns. Standards were run throughout each session. Blanks and off-peak baselines were also determined throughout each analytical session. Selecting and analysing only the highest quality zircons minimised the need for common Pb corrections using measured ^{204}Pb, a procedure made impossible by high ^{204}Hg counts. A single zircon analysis comprises approximately 450 ten-microsecond scans of $^{207}Pb/^{206}Pb$. Ratios reflecting the moving average of twenty ^{207}Pb and ^{206}Pb measurements are first plotted on a graph to check for anomalous ratios throughout a run. Those with high ratios at the beginning are presumed to reflect common Pb and are removed from further consideration. A jump from one ratio plateau to another during one analysis is interpreted to reflect piercing a core or rim of different age. Only data from one plateau at a time were considered. In cases where the beam pierces the grain too deeply and ejecta are not effectively emitted towards the end of an analysis, the signal intensity and commonly also isotope ratios change dramatically. Data from the late part of such runs were also rejected.

With this first assessment of data complete, the ^{207}Pb and ^{206}Pb data were then passed through a 4-sigma filter to remove highly anomalous counts before being passed through a more rigorous 2-sigma filter. The averages of the remaining individual measurements (typically < 5% rejection) of ^{207}Pb and ^{206}Pb provided the final $^{207}Pb/^{206}Pb$ ratio and consequent age. Given the transient signal inherent in LA-ICP-MS and sequential acquisition required by the single collector, standard statistics on multiple blocks of scans is not applicable.

A major limitation of our LA-ICP-MS protocol is that U abundances are not measured; instead only $^{207}Pb/^{206}Pb$ ratios are obtained. A direct indication of concordance is, therefore, not available and all the ages obtained should conservatively be interpreted to represent minimum ages for crystallisation.

A single sample was analysed using the CAMECA IMS 1270 ion microprobe at the NORDSIM laboratory, Naturhistoriska Riksmuseet, Stockholm. The sample was prepared in the same way as the samples analysed by LA-ICP-MS. Reference zircon 91500 from Ontario, Canada, with a weighted average $^{207}Pb/^{206}Pb$ age of 1065 Ma (Wiedenbeck *et al.* 1995), was included in the mount and used as standard. Analytical procedures and common lead corrections are similar to those described by Schuhmacher *et al.* (1994) and Whitehouse *et al.* (1997). Calibrations of Pb/U ratios are based on the observed relationship between Pb/U and UO_2/U and follow procedures similar to those used by the SHRIMP group at the Australian National University (Williams 1998).